Current Biology, Vol. 14, 1–20, December 29, 2004, ©2004 Elsevier Ltd. All rights reserved. DOI 10.1016/j.cub.2004.12.025

Significant Role for p16^{INK4a} in p53-Independent Telomere-Directed Senescence

Jacqueline J.L. Jacobs[1] and Titia de Lange*
Laboratory for Cell Biology and Genetics
The Rockefeller University
1230 York Avenue
New York, NY 10021

Summary

Telomere attrition in primary human fibroblasts induces replicative senescence accompanied by activation of the p53 and p16^{INK4a}/RB tumor suppressor pathways. Although the contribution of p53 and its target, p21, to telomere-driven senescence have been well established, the role of p16^{INK4a} is controversial. Attempts to dissect the significance of p16^{INK4a} in response to telomere shortening have been hampered by the concomitant induction of p16^{INK4a} by cell culture conditions. To circumvent this problem, we studied the role of p16^{INK4a} in the cellular response to acute telomere damage-induced by a dominant negative allele of TRF2, TRF2$^{\Delta B\Delta M}$. This approach avoids the confounding aspects of culture stress because parallel cultures with and without telomere damage can be compared. Telomere damage generated with TRF2$^{\Delta B\Delta M}$ resulted in induction of p16^{INK4a} in the majority of cells as detected by immunohistochemistry. Inhibition of p16^{INK4a} with shRNA or overexpression of BMI1 had a significant effect on the telomere damage response in p53-deficient cells. While p53 deficiency alone only partially abrogated the telomere damage-induced cell cycle arrest, combined inhibition of p16^{INK4a} and p53 led to nearly complete bypass of telomere-directed senescence. We conclude that p16^{INK4a} contributes to the p53-independent response to severe telomere damage.

Results and Discussion

The involvement of p16^{INK4a} in telomere-directed senescence has been contentious [1–10]. Telomere attrition in primary cells induces p16^{INK4a} [11–13], and stabilization of telomeres by telomerase abolishes p16^{INK4a} accumulation [14]. This suggests that p16^{INK4a} is upregulated in response to dysfunctional telomeres and could contribute to telomere-directed senescence. However, p16^{INK4a} also responds to numerous telomere-independent stress signals, including constitutive oncogenic signaling, DNA damage, and suboptimal in vitro tissue culture conditions [4, 15–19]. Previous studies that have addressed the role of p16^{INK4a} in telomere-directed senescence typically relied on prolonged in vitro passaging of cells until they senesce with shortened telomeres. However, by that time cells have not only sustained telomere damage but have also endured extensive stress from in vitro culturing, making it difficult, if not impossible, to specifically address the contribution of p16^{INK4a} to telomere-directed senescence. Here, we avoid this problem and address the role of p16^{INK4a} in telomere-directed senescence independently of additional stresses by inducing immediate telomere dysfunction through inhibition of the telomere binding protein TRF2. When TRF2 is dislodged from telomeres with a dominant negative allele (TRF2$^{\Delta B\Delta M}$), a fraction of chromosome ends lose their protection (reviewed in [20]). The consequences of TRF2 inhibition include degradation of the telomeric 3′ G-overhang by ERCC1/XPF, fusion of chromosome ends by DNA ligase IV, activation of ATM, and recruitment of DNA damage response factors such as 53BP1 and the Mre11 complex to telomeres [21–25]. Loss of the telomeric overhang and association of DNA damage response factors with telomeres have also been observed in fibroblasts that have been passaged into senescence [25, 26].

Fibroblasts respond to this TRF2$^{\Delta B\Delta M}$-induced telomere dysfunction by entering a growth arrest that is indistinguishable from replicative senescence and is accompanied by the activation of p53, induction of p21, upregulation of p16^{INK4a}, and hypophosphorylation of RB [27]. Inhibition of p53 with HPV16E6 or a dominant negative p53 allele (p53^{175H}), or inactivation of RB by HPV16E7 reduces, but does not fully abrogate, this cell cycle arrest [27]. Abrogation of the arrest requires the simultaneous inactivation of both p53 and RB by SV40LT or HPV16E6 and E7 together, suggesting a redundant role for the p53 and RB pathways in the induction of telomere-directed senescence [27]. These studies showed that the RB pathway can mediate telomere-directed cell cycle arrest in a p53-independent manner, but the specific contribution of p16 to this pathway was not addressed.

In order to determine the contribution of p16^{INK4a} to telomere-directed senescence, we used RNAi in combination with TRF2 inhibition in primary human fibroblasts. Prior to induction of telomere damage with TRF2$^{\Delta B\Delta M}$, we introduced p16^{INK4a} shRNA (either one of two different target sequences) and/or p53-repressing reagents according to the schematic shown in Figure 1A. Cells were kept under selective pressure during the course of the analysis to prevent loss of TRF2$^{\Delta B\Delta M}$ expression. Immunofluorescence (IF) detection of TRF2 indicated that all cells retained high levels of TRF2$^{\Delta B\Delta M}$ over the entire 2-week time course of the analysis (Figure 1C and data not shown). Inhibition of p16^{INK4a} with shRNA strongly decreased the expression level of p16^{INK4a} and abolished its induction after telomere damage (Figure 1B). Similarly, repression of p53 with a dominant negative allele (p53^{175H}) or shRNA resulted in diminished p53 activity as detected by impaired induction of p21. The induction of p16^{INK4a} by telomere damage did not require p53.

We reasoned that if p16^{INK4a} is induced by telomere damage in this setting, its expression level should be high in all cells expressing TRF2$^{\Delta B\Delta M}$. We therefore ex-

*Correspondence: delange@mail.rockefeller.edu
[1]Present address: Department of Molecular Genetics, The Netherlands Cancer Institute, Plesmanlaan 121, 1066 CX Amsterdam, The Netherlands.

amined p16^{INK4a} at the cellular level by immunohistochemistry (IHC) under conditions where virtually all cells in the culture express the dominant negative allele of TRF2 (Figure 1C). As expected, p16^{INK4a} was detectable at variable levels in control cells reflecting the occasional induction of p16^{INK4a} by culture conditions. The p16^{INK4a} staining intensity was dramatically increased in cultures expressing TRF2$^{\Delta B\Delta M}$, and this response was seen in nearly every cell. Together with the immunoblotting data, this finding showed that this induction of p16^{INK4a} is a specific response to telomere damage and not the consequence of culture stress.

We next determined the contribution of p16^{INK4a} to the execution of a cell cycle arrest after telomere damage. The normal response to telomere damage is an arrest in G1, which can be monitored by diminished incorporation of BrdU and by lack of cell proliferation [27]. In cells with severely impaired G1/S checkpoints, BrdU incorporation is not diminished after telomere damage. However, such cells still have a growth defect, presumably due to the extensive genome instability resulting from telomere fusions and the concomitant problems in mitosis. As expected from previous studies, inhibition of p53 function with a dominant negative allele (p53^{175H}) or shRNA partially rescued the proliferation block of cells expressing TRF2$^{\Delta B\Delta M}$ (Figures 2A, 2G, and 2H). In addition, p53 inhibition had a strong effect on the rate of BrdU incorporation of cells with telomere damage (Figures 2C, 2E, and 2F). By comparison, the effect of shRNA-mediated p16^{INK4a} inhibition on the proliferation of TRF2$^{\Delta B\Delta M}$-infected cells was not statistically significant (Figure 2). The importance of p53 in mediating the proliferation block after telomere damage was also obvious from TRF2$^{\Delta B\Delta M}$ expression in human fibroblasts that have a homozygous intragenic deletion in the p16^{INK4a} gene [28]. These cells, while lacking p16^{INK4a} function, still displayed a severe proliferation defect and diminished BrdU incorporation after introduction of TRF2$^{\Delta B\Delta M}$ (Figure 2D and data not shown). Thus, p16^{INK4a} deficiency alone does not allow a strong by-pass of the telomere damage-induced arrest.

Although p53 deficiency had an obvious impact on the TRF2$^{\Delta B\Delta M}$-induced proliferation block, the effect was always partial, even when p53 was inhibited with shRNA. Because this result suggested the presence of a p53-independent response to telomere damage, we examined the role of p16^{INK4a} in this setting. By determining the rate of BrdU incorporation in TRF2$^{\Delta B\Delta M}$ cultures relative to the appropriate vector control cultures, we corrected for the effects of p16^{INK4a} and p53 inhibition on entry into S phase in the absence of TRF2$^{\Delta B\Delta M}$. This approach removes possible effects of culture stress and allows specific evaluation of the role of p16^{INK4a} in the telomere dysfunction-induced G1/S arrest. The corrected data showed that whereas inhibition of p53 afforded a partial escape from TRF2$^{\Delta B\Delta M}$-induced growth arrest, inhibition of both p16^{INK4a} and p53 together resulted in an almost complete restoration of the rate of DNA synthesis (Figures 2E and 2F; $p = 1.32x10^{-9}$ [$n = 17$] for the relative effect of p16sh in p53^{175H} cells). This indicates that in absence of p53, p16^{INK4a} is an inhibitor of entry into S phase after telomere damage.

Immunofluorescence analysis of TRF2 expression

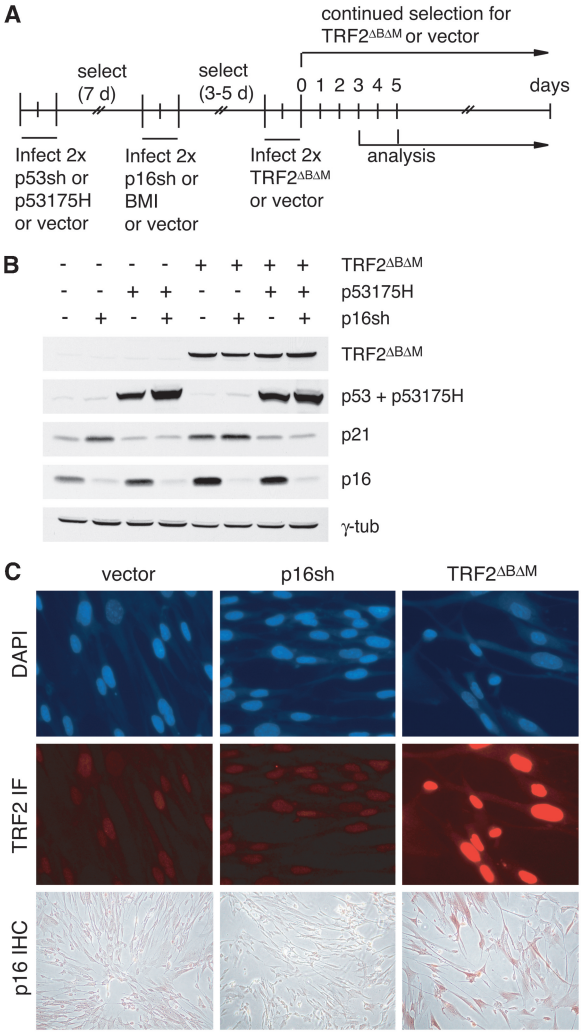

Figure 1. Induction of p16^{INK4a} upon TRF2$^{\Delta B\Delta M}$-Mediated Telomere Dysfunction

(A) Experimental set-up: IMR90 primary human fibroblasts were sequentially transduced with 1) pBabeNeo-P53^{175H}, pRetroSuper-p53sh, or appropriate empty vector control, 2) pRetroSuper-p16sh, MSCVU6-p16sh, pBabePuro-BMI1, or corresponding vector control, 3) pBabePuro-TRF2$^{\Delta B\Delta M}$, pWZLHygro-TRF2$^{\Delta B\Delta M}$, or corresponding vector control. The data shown in Figure 2 was obtained with pRetroSuper-p16sh. MSCVU6-p16sh gave similar results. After each round of infection, cells were first passaged in medium containing neomycin, hygromycin, or puromycin for 7, 4–5, or 3 days, respectively, before continuing with the next round of infection. After the final infection with TRF2$^{\Delta B\Delta M}$, cells were kept in selective medium during the analysis to prevent loss of the TRF2$^{\Delta B\Delta M}$ retrovirus.

(B) Expression of TRF2$^{\Delta B\Delta M}$, p53^{175H}, p21, and p16^{INK4a} proteins in IMR90 cells infected with combinations of empty vector, p16sh-(pRetroSuper), p53^{175H}-, and TRF2$^{\Delta B\Delta M}$-encoding retroviruses. Lysates were prepared on day 17 and equal amounts of protein were loaded in each lane (immunoblotting for γ-tubulin serves as loading control). At the time point analyzed, the previously documented induction of endogenous p53 by TRF2$^{\Delta B\Delta M}$ is no longer detectable.

(C) Immunohistochemical analysis of p16^{INK4a} and detection of TRF2$^{\Delta B\Delta M}$ by immunofluorescence in primary IMR90 fibroblasts infected with control, p16sh-, or TRF2$^{\Delta B\Delta M}$-encoding retroviruses on day 8. Data shown are with pRetroSuper-p16sh. MSCVU6-p16sh gave the same result.

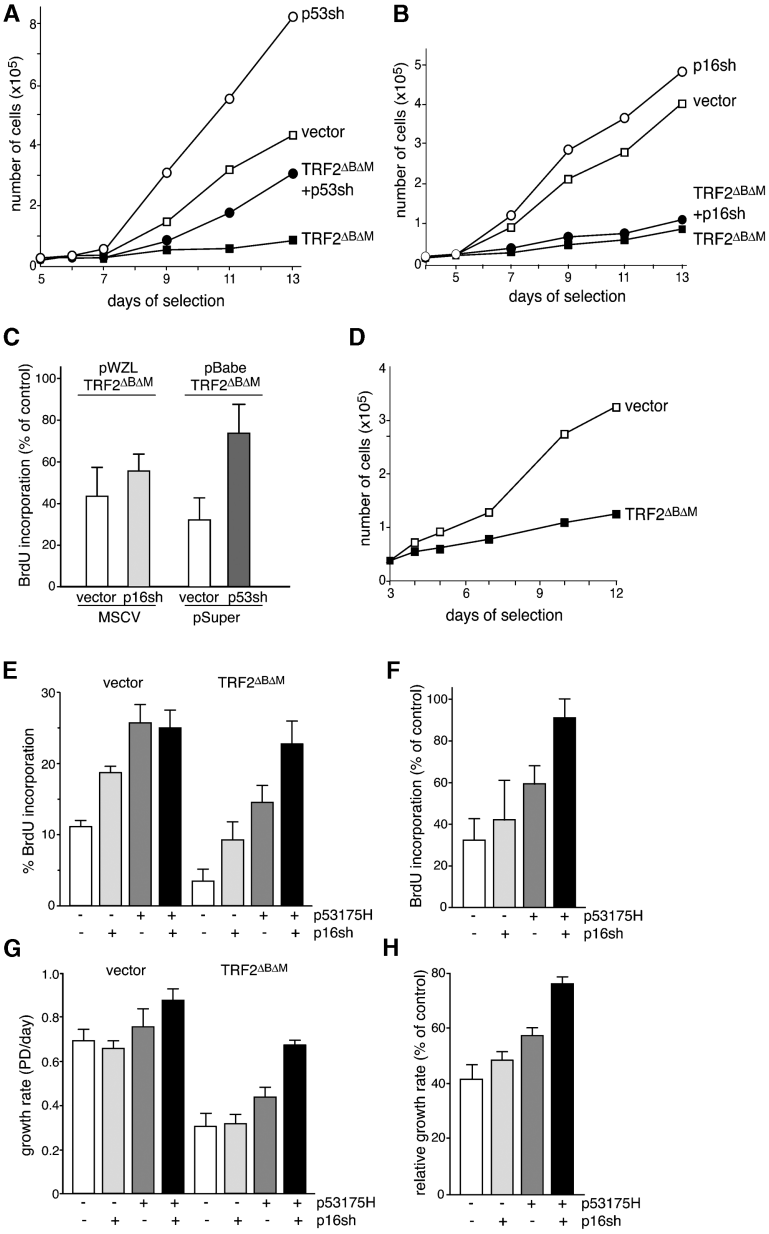

Figure 2. Inhibition of p16^{INK4a} Cooperates with p53 Inactivation in Abrogating TRF2$^{\Delta B\Delta M}$-Induced Growth Arrest

(A) Inhibition of p53 alone partially alleviates TRF2$^{\Delta B\Delta M}$–induced growth arrest. Growth curves of IMR90 primary human fibroblasts infected with pRetroSuper-p53sh and/or pBabePuro-TRF2$^{\Delta B\Delta M}$ retroviruses. Standard deviations were less than 10%.

(B) Inhibition of p16 alone does not significantly improve the proliferation of cells with TRF2$^{\Delta B\Delta M}$-induced telomere damage. Growth curves of IMR90 cells infected with MSCVU6-p16sh and/or pWZLH-TRF2$^{\Delta B\Delta M}$ retroviruses. Standard deviations were less than 10%.

(C) S phase index in TRF2$^{\Delta B\Delta M}$-espressing IMR90 cells shown in (A) and (B) measured by BrdU incorporation on day 8.

(D) Growth curves of p16^{INK4a}-deficient human diploid fibroblasts after infection with a pBabePuro-TRF2$^{\Delta B\Delta M}$ retrovirus. Standard deviations were less than 10%

(E) BrdU incorporation rates (on day 8) of primary IMR90 fibroblasts infected with pBabe-Neo-p53^{175H} or pBabe-Neo control and pRetroSuper-p16sh or pRetroSuper control retroviruses followed by pBabePuro-TRF2$^{\Delta B\Delta M}$ or pBabePuro control retroviruses.

(F) Relative BrdU incorporation rates of primary IMR90 fibroblasts infected with combinations of vector control, p53^{175H}-, and p16sh-encoding retroviruses. Averages from three independent experiments using two different p16sh vectors (pRetroSuper-p16sh and MSCVU6-p16sh) are shown.

(G) Growth rates of IMR90 cells infected with pBabeNeo-p53^{175H} or pBabeNeo control and pRetroSuper-p16sh or pRetroSuper control followed by pBabePuro-TRF2$^{\Delta B\Delta M}$ or pBabePuro control retroviruses. Growth rates were determined by calculating the average increase in population doublings over days 3–11 of selection from five experiments (three independent infections).

(H) Growth rates of TRF2$^{\Delta B\Delta M}$-espressing cells in G, relative to their respective vector controls.

confirmed that the observed rescue in DNA synthesis by combined p53 and p16^{INK4a} inhibition was not due to an increased outgrowth of cells with diminished TRF2$^{\Delta B\Delta M}$ expression (Figure 1C and data not shown). On the contrary, TRF2$^{\Delta B\Delta M}$ expression levels appeared higher in cells with inhibited p53 and p16^{INK4a} expression than in controls, especially at later time points when controls cells showed decreased TRF2$^{\Delta B\Delta M}$ expression (data not shown). This suggests a greater tolerance for telomere damage and thus less selection against TRF2$^{\Delta B\Delta M}$ in cells lacking both p53 and p16^{INK4a} function.

To assess the effect of p16^{INK4a} on the proliferation of p53 deficient cells with telomere damage, we measured culture growth rates during the 2 weeks following infection with the TRF2$^{\Delta B\Delta M}$ retrovirus. Cultures were not followed longer because after 2–3 weeks, cells with lowered levels of TRF2$^{\Delta B\Delta M}$ begin to appear. TRF2$^{\Delta B\Delta M}$ expression resulted in a 60% reduction in proliferation of IMR90 fibroblasts (Figures 2G–2H). Whereas inhibition of p53 alone resulted in partial rescue of TRF2$^{\Delta B\Delta M}$-induced growth arrest, a significantly better rescue was observed in cultures in which both p16^{INK4a} and p53 were inactivated ($p = 1.30x10^{-6}$ [$n = 5$] for the relative effect of pRetroSuper-p16sh in p53^{175H} cells in Figure 2H; $p = 0.0196$ [$n = 3$] for the relative effect of a second shRNA, MSCVU6-p16sh in p53^{175H} cells [data not shown]).

Although the rescue of DNA synthesis by combined inactivation of p16^{INK4a} and p53 was almost complete (~90%; Figure 2F), the cells still showed a somewhat reduced proliferation rate (70%–80%; Figure 2H). This can be explained by the deleterious effects of telomere fusions, which include anaphase bridges, chromosome nondisjunction, translocations, and deletions [22]. So even though the downstream signaling response to telo-

Table 1. Chromosome Fusions in IMR90 Cells Expressing TRF2$^{\Delta B\Delta M}$

Retroviruses	% Metaphases with Chromosome Fusions	Number of Fusion per Metaphase
vector	0 (n = 35)	0
TRF2$^{\Delta B\Delta M}$	37 (n = 27)	0.56
TRF2$^{\Delta B\Delta M}$ + p16sh	41 (n = 22)	0.55
TRF2$^{\Delta B\Delta M}$ + p53175H	64 (n = 22)	1.68
TRF2$^{\Delta B\Delta M}$ + p16sh + p53175H	53 (n = 30)	1.33
TRF2$^{\Delta B\Delta M}$ + BMI1 + p53175H	60 (n= 20)	2.0

mere dysfunction might be disabled through p53 and p16^{INK4a} inactivation, telomere damage still results in lethal genome instability. Indeed, metaphase spreads of TRF2$^{\Delta B\Delta M}$-expressing cells with inhibited p16^{INK4a} and p53 function contained multiple chromosome end fusions (Table 1). This excludes the fact that the observed p16/p53-mediated rescue of the growth arrest induced by TRF2$^{\Delta B\Delta M}$ is due to improved telomere protection. In fact, the frequency of chromosome fusions in cells with inhibited p16^{INK4a} and p53 function, as well as in TRF2$^{\Delta B\Delta M}$-expressing cells with inactivated p53 only, was higher than in TRF2$^{\Delta B\Delta M}$-expressing cells with normal p53 and p16^{INK4a} function. This is consistent with our observations that these cells have a diminished ability to arrest in response to TRF2$^{\Delta B\Delta M}$-induced telomere dysfunction.

Besides growth arrest and upregulation of cell cycle inhibitors, other characteristics of senescent cells are their flat morphology and staining for senescence-associated β-galactosidase (SA-β-galactosidase) [29]. Although a significant reduction in these parameters was seen, especially for p53^{175H} cultures, flat and SA-β-galactosidase positive cells were still observed in p53^{175H} or p16sh IMR90 cultures expressing TRF2$^{\Delta B\Delta M}$ (Figure 3). However, TRF2$^{\Delta B\Delta M}$-expressing cultures in which both p53 and p16^{INK4a} were inhibited were morphologically indistinguishable from control cultures and negative for SA-β-galactosidase activity (Figure 3). This result further illustrates that in absence of p53, p16^{INK4a} has an important role in inducing senescence in response to telomere damage.

As an independent way of inhibiting p16^{INK4a}, we expressed the Polycomb-group repressor BMI1 alone and in combination with p53^{175H} in IMR90 fibroblasts and investigated the response to TRF2$^{\Delta B\Delta M}$. BMI1 represses the expression of both p16^{INK4a} and the second product of the INK4a locus p19^{ARF} and has been shown to extend the replicative lifespan of mouse and human fibroblasts [6, 30]. BMI1 prevented the induction of p16^{INK4a} upon TRF2$^{\Delta B\Delta M}$ expression, indicating that increased Polycomb-group repression on the INK4a locus is dominant over the mechanism that drives p16 upregulation upon telomere dysfunction (Figure 4A).Consistent with our results from using RNA interference to inhibit p16^{INK4a}, BMI1 significantly reduced the proliferation-inhibiting effect of TRF2$^{\Delta B\Delta M}$, especially in combination with p53 inhibition (Figures 4B–4D).

Telomere-directed senescence is regarded as a major tumor suppressor mechanism by limiting the outgrowth of potentially tumorigenic cells (reviewed in [31–34]). Telomeres whose functionality has been compromised as a result of extensive attrition of telomeric DNA or due to reduced function of telomere capping proteins behave like chromosome internal double-strand breaks,

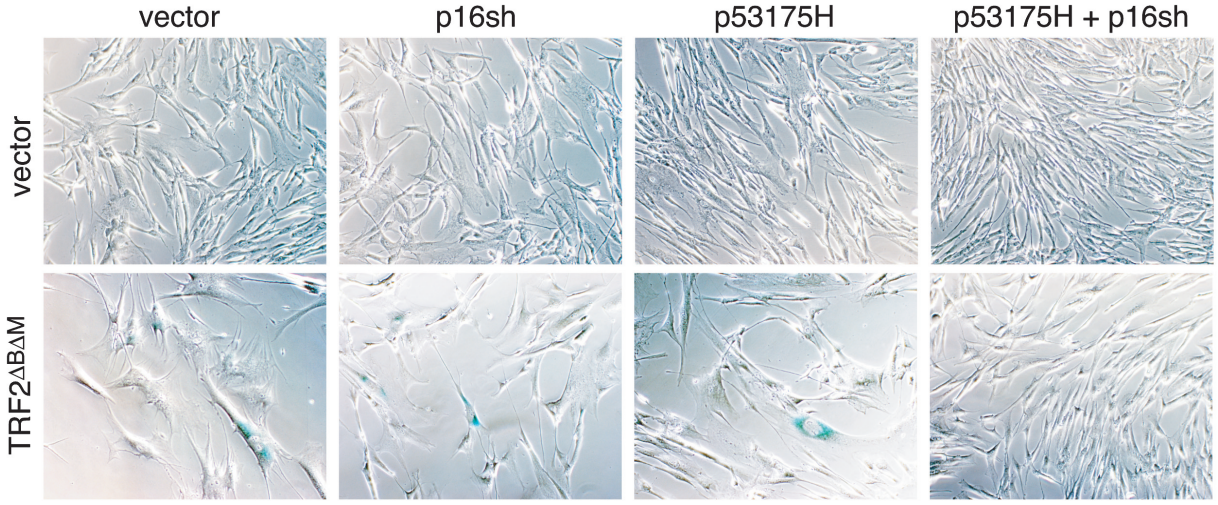

Figure 3. Inhibition of Both p53 and p16^{INK4a} Abolishes Senescent Morphology and SA-β-Galactosidase Activity in Primary IMR90 Fibroblasts with Dysfunctional Telomeres

IMR90 primary fibroblasts infected with combinations of empty vector control, p53^{175H}-, p16sh- (pRetroSuper), or TRF2$^{\Delta B\Delta M}$-encoding retroviruses and stained for SA-β-galactosidase activity at day 12.

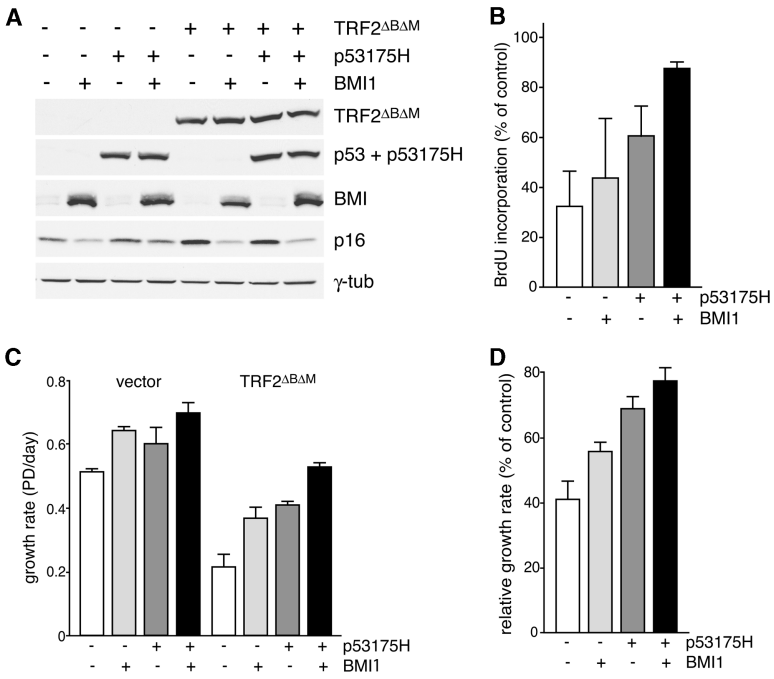

Figure 4. The p16^{INK4a}-Repressor BMI1 Attenuates the Senescence Response to TRF2$^{\Delta B\Delta M}$

(A) P53^{175H}, BMI1, TRF2$^{\Delta B\Delta M}$, and p16^{INK4a} protein levels in IMR90 cells shown in (B)–(D) at day 12 of selection. Equal amounts of protein were loaded in each lane.

(B) S phase index of primary IMR90 fibroblasts infected with combinations of control, BMI1-, p53^{175H}-, and TRF2$^{\Delta B\Delta M}$-encoding retroviruses at day 8 of selection. The averages of two independent experiments are shown.

(C) Average growth rates of IMR90 fibroblasts infected with BMI1- and/or p53^{175H}-encoding retroviruses followed by pWZLH or pWZLH-TRF2$^{\Delta B\Delta M}$. Growth rates were determined over days 4–12 from three duplicate experiments (two independent infections).

(D) Relative growth rates of IMR90 fibroblasts in which p16^{INK4a} was repressed by BMI1 and p53 was inhibited by p53^{175H} expression or shRNA. Graph represents results from three independent duplicate experiments.

resulting in cell cycle arrest and senescence or apoptosis. In cells with impaired DNA damage response checkpoints, dysfunctional telomeres can induce genome instability and a complex spectrum of genetic alterations that promotes tumorigenesis (reviewed in [32, 35]). Recent data provided evidence for loss of telomere function and the associated genome instability early in human breast cancer at the transition to ductal carcinoma in situ [36]. These considerations underscore the need for detailed understanding of the cellular response to deprotected telomeres.

Here, we have used TRF2 inhibition as a tool to induce immediate telomere dysfunction in order to specifically address the contribution of the p53 and p16^{INK4a}/RB pathways to the telomere damage response. We found that p53 plays a major role but that p16^{INK4a} is also clearly responsible for a substantial part of telomere-directed senescence in primary human fibroblasts. Thus, p16^{INK4a} provides an important additional fail-safe that prevents unlimited proliferation in the presence of telomere damage even when the p53 pathway is disrupted. A similar observation was made recently in a study on the reversibility of human cellular senescence, in which it was found that p53 inactivation only resulted in the reversal of senescence in cells with low levels of p16^{INK4a} and not in cells with high levels of p16^{INK4a} [37]. However, in that study, as well as in a different study addressing the contribution of p16^{INK4a} to senescence by transient transfection of siRNA [8], cells were extensively passaged until a senescent state was reached. Therefore, the p16^{INK4a} response probably at least in part reflects a reaction to accumulated culture stress and does not directly address the role of p16^{INK4a} in the telomere damage pathway.

Although the effect of p16 inhibition on TRF2$^{\Delta B\Delta M}$-induced growth arrest in p53-deficient cells is very clear, the effect was minimal in p53 proficient cells. We cannot exclude that this is in part related to the use of TRF2$^{\Delta B\Delta M}$ as a surrogate for telomere shortening. For instance, our strategy forces us to analyze relatively early time points at which p16 might not yet be at its maximum due to its slow induction, resulting in the predominance of the faster p53-dependent response.

A recent study of replicative senescence at the single-cell level concluded that p16^{INK4a} is not involved in senescence triggered by telomere shortening [9], a conclusion that is discordant with the findings reported here. This conclusion was based on the lack of a correlation between the presence of γ-H2AX foci (an indicator of telomere dysfunction) and upregulation of p16^{INK4a}, whereas this correlation did exist for p21. However, the formation of γ-H2AX foci and the induction of p16^{INK4a} occur with different kinetics. DNA damage foci are formed immediately (within hours) after telomere deprotection and they are transient [23, 38]. By contrast, the induction of p16^{INK4A} after telomere dysfunction appears to be a very slow process. After retroviral infection of TRF2$^{\Delta B\Delta M}$, it takes one or two weeks before p16^{INK4a} is readily detectable, a time point at which the γ-H2AX foci will have disappeared. Therefore, it would be expected that cells with high levels of p16^{INK4a} are generally devoid of γ-H2AX foci and vice versa, explaining the lack of correlation observed. Thus, our finding that p16^{INK4a} is a significant mediator of telomere-directed senescence is not necessarily in conflict with the data of Herbig et al. [9].

The signal through which dysfunctional telomeres activate p53 and RB has not been fully established; however, the telomere damage response has the hallmarks of a DNA damage response and is transmitted through the ATM and ATR kinases [23, 25, 39]. The resulting activation of p53 by phosphorylation leads to increased expression of p21, which activates RB family proteins by inhibiting their phosphorylation by cyclin dependent kinases [40]. Targeted disruption of p21 alone has been

shown to be sufficient to abolish senescence in human fibroblasts [41]. In our study, inactivation of p53, which prevents the p53-mediated increase in p21, only partially abrogated TRF2$^{\Delta B\Delta M}$-induced senescence and full bypass required the concomitant inhibition of p16^{INK4a}. These data can be reconciled with the full bypass of senescence in the p21 knockout cells by the arguement that p16^{INK4a} acts largely through the release of basal levels of p21 from CDK4 and CDK6 [42–44].

A remaining challenge will be to determine what the signal is that leads to activation of p16^{INK4a} after telomere dysfunction. The activation of p16^{INK4a} appears to be independent of ATM because A-T cells are not compromised in their p16^{INK4a} response to telomere dysfunction [23]. It is likely that the induction of p16^{INK4a} differs significantly from the pathway that activates p53 because p53 and p21 are induced rapidly after telomere damage, whereas the kinetics of the p16^{INK4a} response is very slow. Similar slow kinetics have also been reported for activation of p16^{INK4a} after global DNA damage, e.g., as a consequence of γ-irradiation, UV or DNA double-strand break inducing agents [16–19], and it is very well possible that telomere damage and other forms of DNA damage activate p16^{INK4a} through a similar pathway.

Experimental Procedures

Standard assay conditions and retroviral gene delivery techniques were employed. For details, see Supplemental Data.

Supplemental Data

Supplemental Data including Experimental Procedures are available at http://www.current-biology.com/cgi/content/full/14/24/■■■/DC1/.

Acknowledgments

We thank R. Agami for pRetroSuper-p53sh and pRetroSuper-p16sh vectors, S. Lowe for MSCVU6-p16sh vector, M. van Lohuizen for PBP-BMI1 and LZRS-BMI1 vectors and F6 antibody, and G. Peters for p16^{INK4a}-deficient cells. J.J. was supported by a Dutch Cancer Society Fellowship. This work was supported by a National Institutes of Health grant to T.dL. (AG16642).

Received: September 17, 2004
Revised: October 19, 2004
Accepted: October 20, 2004
Published: December 29, 2004

References

1. Kiyono, T., Foster, S.A., Koop, J.I., McDougall, J.K., Galloway, D.A., and Klingelhutz, A.J. (1998). Both Rb/p16INK4a inactivation and telomerase activity are required to immortalize human epithelial cells. Nature *396*, 84–88.
2. Dickson, M.A., Hahn, W.C., Ino, Y., Ronfard, V., Wu, J.Y., Weinberg, R.A., Louis, D.N., Li, F.P., and Rheinwald, J.G. (2000). Human keratinocytes that express hTERT and also bypass a p16(INK4a)- enforced mechanism that limits life span become immortal yet retain normal growth and differentiation characteristics. Mol. Cell. Biol. *20*, 1436–1447.
3. Munro, J., Steeghs, K., Morrison, V., Ireland, H., and Parkinson, E.K. (2001). Human fibroblast replicative senescence can occur in the absence of extensive cell division and short telomeres. Oncogene *20*, 3541–3552.
4. Ramirez, R.D., Morales, C.P., Herbert, B.S., Rohde, J.M., Passons, C., Shay, J.W., and Wright, W.E. (2001). Putative telomere-independent mechanisms of replicative aging reflect inadequate growth conditions. Genes Dev. *15*, 398–403.
5. Morris, M., Hepburn, P., and Wynford-Thomas, D. (2002). Sequential extension of proliferative lifespan in human fibroblasts induced by over-expression of CDK4 or 6 and loss of p53 function. Oncogene *21*, 4277–4288.
6. Itahana, K., Zou, Y., Itahana, Y., Martinez, J.L., Beausejour, C., Jacobs, J.J., Van Lohuizen, M., Band, V., Campisi, J., and Dimri, G.P. (2003). Control of the replicative life span of human fibroblasts by p16 and the polycomb protein Bmi-1. Mol. Cell. Biol. *23*, 389–401.
7. Wei, W., Herbig, U., Wei, S., Dutriaux, A., and Sedivy, J.M. (2003). Loss of retinoblastoma but not p16 function allows bypass of replicative senescence in human fibroblasts. EMBO Rep. *4*, 1061–1066.
8. Bond, J., Jones, C., Haughton, M., DeMicco, C., Kipling, D., and Wynford-Thomas, D. (2004). Direct evidence from siRNA-directed "knock down" that p16(INK4a) is required for human fibroblast senescence and for limiting ras-induced epithelial cell proliferation. Exp. Cell Res. *292*, 151–156.
9. Herbig, U., Jobling, W.A., Chen, B.P., Chen, D.J., and Sedivy, J.M. (2004). Telomere shortening triggers senescence of human cells through a pathway involving ATM, p53, and p21(CIP1), but not p16(INK4a). Mol. Cell *14*, 501–513.
10. Brookes, S., Rowe, J., Gutierrez Del Arroyo, A., Bond, J., and Peters, G. (2004). Contribution of p16(INK4a) to replicative senescence of human fibroblasts. Exp. Cell Res. *298*, 549–559.
11. Hara, E., Smith, R., Parry, D., Tahara, H., Stone, S., and Peters, G. (1996). Regulation of p16CDKN2 expression and its implications for cell immortalization and senescence. Mol. Cell. Biol. *16*, 859–867.
12. Alcorta, D.A., Xiong, Y., Phelps, D., Hannon, G., Beach, D., and Barrett, J.C. (1996). Involvement of the cyclin-dependent kinase inhibitor p16 (INK4a) in replicative senescence of normal human fibroblasts. Proc. Natl. Acad. Sci. USA *93*, 13742–13747.
13. Palmero, I., McConnell, B., Parry, D., Brookes, S., Hara, E., Bates, S., Jat, P., and Peters, G. (1997). Accumulation of p16INK4a in mouse fibroblasts as a function of replicative senescence and not of retinoblastoma gene status. Oncogene *15*, 495–503.
14. Bodnar, A.G., Ouellette, M., Frolkis, M., Holt, S.E., Chiu, C.P., Morin, G.B., Harley, C.B., Shay, J.W., Lichtsteiner, S., and Wright, W.E. (1998). Extension of life-span by introduction of telomerase into normal human cells Science *279*, 349–352.
15. Serrano, M., Lin, A.W., McCurrach, M.E., Beach, D., and Lowe, S.W. (1997). Oncogenic ras provokes premature cell senescence associated with accumulation of p53 and p16INK4a. Cell *88*, 593–602.
16. Robles, S.J., and Adami, G.R. (1998). Agents that cause DNA double strand breaks lead to p16INK4a enrichment and the premature senescence of normal fibroblasts. Oncogene *16*, 1113–1123.
17. Shapiro, G.I., Edwards, C.D., Ewen, M.E., and Rollins, B.J. (1998). p16INK4A participates in a G1 arrest checkpoint in response to DNA damage. Mol. Cell. Biol. *18*, 378–387.
18. Piepkorn, M. (2000). The expression of p16(INK4a), the product of a tumor suppressor gene for melanoma, is upregulated in human melanocytes by UVB irradiation. J. Am. Acad. Dermatol. *42*, 741–745.
19. te Poele, R.H., Okorokov, A.L., Jardine, L., Cummings, J., and Joel, S.P. (2002). DNA damage is able to induce senescence in tumor cells in vitro and in vivo. Cancer Res. *62*, 1876–1883.
20. de Lange, T. (2002). Protection of mammalian telomeres. Oncogene *21*, 532–540.
21. van Steensel, B., Smogorzewska, A., and de Lange, T. (1998). TRF2 protects human telomeres from end-to-end fusions. Cell *92*, 401–413.
22. Smogorzewska, A., Karlseder, J., Holtgreve-Grez, H., Jauch, A., and de Lange, T. (2002). DNA Ligase IV-Dependent NHEJ of Deprotected Mammalian Telomeres in G1 and G2. Curr. Biol. *12*, 1635–1644.
23. Takai, H., Smogorzewska, A., and de Lange, T. (2003). DNA damage foci at dysfunctional telomeres. Curr. Biol. *13*, 1549–1556.
24. Zhu, X.D., Niedernhofer, L., Kuster, B., Mann, M., Hoeijmakers, J.H., and de Lange, T. (2003). ERCC1/XPF Removes the 3′ Over-

hang from Uncapped Telomeres and Represses Formation of Telomeric DNA-Containing Double Minute Chromosomes. Mol. Cell *12*, 1489–1498.
25. d'Adda di Fagagna, F., Reaper, P.M., Clay-Farrace, L., Fiegler, H., Carr, P., Von Zglinicki, T., Saretzki, G., Carter, N.P., and Jackson, S.P. (2003). A DNA damage checkpoint response in telomere-initiated senescence. Nature *426*, 194–198.
26. Stewart, S.A., Ben-Porath, I., Carey, V.J., O'Connor, B.F., Hahn, W.C., and Weinberg, R.A. (2003). Erosion of the telomeric single-strand overhang at replicative senescence. Nat. Genet. *33*, 492–496.
27. Smogorzewska, A., and de Lange, T. (2002). Different telomere damage signaling pathways in human and mouse cells. EMBO J. *21*, 4338–4348.
28. Brookes, S., Rowe, J., Ruas, M., Llanos, S., Clark, P.A., Lomax, M., James, M.C., Vatcheva, R., Bates, S., Vousden, K.H., et al. (2002). INK4a-deficient human diploid fibroblasts are resistant to RAS-induced senescence. EMBO J. *21*, 2936–2945.
29. Dimri, G.P., Lee, X., Basile, G., Acosta, M., Scott, G., Roskelley, C., Medrano, E.E., Linskens, M., Rubelj, I., Pereira-Smith, O., et al. (1995). A biomarker that identifies senescent human cells in culture and in aging skin in vivo. Proc. Natl. Acad. Sci. USA *92*, 9363–9367.
30. Jacobs, J.J., Kieboom, K., Marino, S., DePinho, R.A., and van Lohuizen, M. (1999). The oncogene and Polycomb-group gene bmi-1 regulates cell proliferation and senescence through the ink4a locus. Nature *397*, 164–168.
31. Campisi, J. (2001). Cellular senescence as a tumor-suppressor mechanism. Trends Cell Biol. *11*, S27–S31.
32. Maser, R.S., and DePinho, R.A. (2002). Connecting chromosomes, crisis, and cancer. Science *297*, 565–569.
33. Sharpless, N.E., and DePinho, R.A. (2004). Telomeres, stem cells, senescence, and cancer. J. Clin. Invest. *113*, 160–168.
34. Itahana, K., Campisi, J., and Dimri, G.P. (2004). Mechanisms of cellular senescence in human and mouse cells. Biogerontology *5*, 1–10.
35. de Lange, T. (1995). Telomere dynamics and genome instability in human cancer. In Telomeres, E.H.B.a.C.W. Greider, ed. (CSH: CSH press), pp. 265–293.
36. Chin, K., De Solorzano, C.O., Knowles, D., Jones, A., Chou, W., Rodriguez, E.G., Kuo, W.L., Ljung, B.M., Chew, K., Myambo, K., et al. (2004). In situ analyses of genome instability in breast cancer. Nat. Genet. *36*, 984–988.
37. Beausejour, C.M., Krtolica, A., Galimi, F., Narita, M., Lowe, S.W., Yaswen, P., and Campisi, J. (2003). Reversal of human cellular senescence: roles of the p53 and p16 pathways. EMBO J. *22*, 4212–4222.
38. Bakkenist, C.J., Drissi, R., Wu, J., Kastan, M.B., and Dome, J.S. (2004). Disappearance of the telomere dysfunction-induced stress response in fully senescent cells. Cancer Res. *64*, 3748–3752.
39. Karlseder, J., Broccoli, D., Dai, Y., Hardy, S., and de Lange, T. (1999). p53- and ATM-dependent apoptosis induced by telomeres lacking TRF2. Science *283*, 1321–1325.
40. Sherr, C.J., and Roberts, J.M. (1999). CDK inhibitors: positive and negative regulators of G1-phase progression. Genes Dev. *13*, 1501–1512.
41. Brown, J.P., Wei, W., and Sedivy, J.M. (1997). Bypass of senescence after disruption of p21CIP1/WAF1 gene in normal diploid human fibroblasts. Science *277*, 831–834.
42. Mitra, J., Dai, C.Y., Somasundaram, K., El-Deiry, W.S., Satyamoorthy, K., Herlyn, M., and Enders, G.H. (1999). Induction of p21(WAF1/CIP1) and inhibition of Cdk2 mediated by the tumor suppressor p16(INK4a). Mol. Cell. Biol. *19*, 3916–3928.
43. McConnell, B.B., Gregory, F.J., Stott, F.J., Hara, E., and Peters, G. (1999). Induced expression of p16(INK4a) inhibits both CDK4- and CDK2- associated kinase activity by reassortment of cyclin-CDK-inhibitor complexes. Mol. Cell. Biol. *19*, 1981–1989.
44. Parry, D., Mahony, D., Wills, K., and Lees, E. (1999). Cyclin D-CDK subunit arrangement is dependent on the availability of competing INK4 and p21 class inhibitors. Mol. Cell. Biol. *19*, 1775–1783.

Supplemental Data

Significant Role for p16^{INK4a} in p53-Independent Telomere-Directed Senescence

Jacqueline J.L. Jacobs and Titia de Lange

Supplemental Experimental Procedures

Retroviral Infections

IMR90 primary human fibroblasts and amphotropic phoenix retroviral producer cells (both from ATCC) were grown in DMEM with 100 U of penicillin, 0.1 mg/ml streptomycin, 2 mM L-glutamine, 0.1 mM non-essential amino acids and 15% FBS (10% FBS for phoenix). For production of retroviral stocks, phoenix cells were seeded at 3×10^6 cells/10 cm dish and transfected using CaPO4 precipitation of 50 μg of DNA. Medium was refreshed at 16 and 24 hr after adding the DNA/$CaPO_4$ precipitate and viral supernatants were harvested, filtered through a 0.45 μM syringe filter at approximately 48, 62, and 72 hr posttransfection. Viral supernatants were either frozen on dry ice and stored at -80°C until use or used immediately. For infection IMR90 cells were overlaid with viral supernatant supplemented with 4 μg/ml polybrene and 5% FBS. After 8 hr 1 volume of fresh medium was added and cells were incubated for an additional 16 hr after which a second infection was started. 24 hr after the second infection cells were trypsinized and plated in appropriate selection medium. Typically 95%–100% of the cells were infected and drug resistant. After selection was completed cells were subjected to additional rounds of infections with different viruses. PBabePuro-TRF2$^{\Delta B\Delta M}$ and pWZLH-TRF2$^{\Delta B\Delta M}$ were described before [S1]. pBabeNeo-p53^{175H} was generated by cloning human p53^{175H} cDNA [S2] into pBabeNeo. pBabePuro-BMI1 and LZRS-BMI1 were gifts from M. van Lohuizen [S3, S4]. pRetroSuperHygro-p53sh and pRetroSuperHygro-p16sh were gifts from R. Agami [S5, S6]. MSCVPuroU6-p16sh was provided by S. Lowe [S7].

Growth Curves, BrdU Labeling, and SA-β-Gal Assay

For growth curves, cells were plated in 12-wells plates at 20,000 cells/well and on subsequent days the amount of cells in each of duplicate or triplicate wells were counted. The increase in population doublings was plotted against time and the slope of the curves was taken as a measure for the rate of proliferation. Late time points, at which one or more cultures became very dense and contact-inhibited, were excluded from the analysis for all cultures within the experiment. BrdU incorporation assays were performed by plating cells on coverslips a minimum of 2 days prior to the assay. Cells were incubated in 10 μM BrdU for 1 hr, washed twice in PBS, fixed in 5% acetic acid/95% ethanol for 15 min at -20°C, incubated twice for 5 min in PBS, for 20 min in 2 M HCl/0.5% Triton-X-100, washed 4 times 5 min in PBS and incubated for 30 min in 0.2% cold water fish gelatin, 0.5% BSA in PBS (PBG). Following a 2 hr incubation with anti-TRF2 Ab 647 polyclonal (1:2000, [S8]) and anti-BrdU monoclonal (Dako, 1:10) antibodies in PBG, coverslips were washed 3 times 5 min in PBS and incubated for 45 min with TRITC-conjugated donkey anti-rabbit and FITC-conjugated sheep anti-mouse antibodies (Jackson) in PBG. After 3 washes in PBS, DNA was counterstained with DAPI and coverslips were mounted in Vectastain (Vector Labs). The percentage of BrdU positive cells was determined from a minimum of 400 cells for each culture. Immunofluorescence detection of TRF2 indicated that all cells expressed TRF2$^{\Delta B\Delta M}$. P-values for the statistical evaluation of differences in growth rates or S-phase indices were determined according to Student's-t test (two-tailed). Staining for SA-β-Gal activity was performed as described [S9].

Immunofluorescence, Immunohistochemistry, Immunoblotting, and Metaphase Chromosome Analysis

Immunofluorescence detection of TRF2 was done on acetic acid/ethanol or paraformaldehyde fixed slides essentially as described for the BrdU incorporation assay but eliminating the denaturation step. Immunohistochemical detection of p16^{INK4a} was performed on acetic acid/ethanol fixed slides using antibody JC8 (Abcam) as described [S10]. Whole cell lysates were prepared in RIPA lysis buffer (150 mM NaCl, 1% NP40, 0.1% SDS, 0.5% DOC, 50 mM Tris-Hcl pH 8, 2 mM EDTA pH 8, 0.2 mM PMSF, 0.5 mM DTT) and equal amounts of protein were fractionated on SDS-PAGE and blotted onto nitrocellulose. Immunoblotting was according to standard methods using enhanced chemiluminescence (ECL kit Amersham). Membranes were blocked overnight at 4°C in 5% milk/0.1% Tween in PBS, primary and secondary antibody incubations were in 1% milk/0.1% Tween in PBS for p16^{INK4a} (C-20, Santa Cruz Biotechnology), TRF2 (647, [S8]), BMI1 (F6, [S11]) and γ-tubulin (GTU88, Sigma). For p21 (F-5, Santa Cruz Biotechnology) and p53 (DO-1, Santa Cruz Biotechnology) antibody incubations were in 5% milk/0.1% Tween. For metaphase chromosome analysis, cells were incubated with colcemid for 6 hr on day 6. Cell harvesting and preparation of metaphase spreads were performed as described previously [S12]. DNA was stained with DAPI and spreads were carefully analyzed for the presence of chromosomal fusions.

Supplemental References

S1. Smogorzewska, A., and de Lange, T. (2002). Different telomere damage signaling pathways in human and mouse cells. EMBO J. *21*, 4338–4348.

S2. Baker, S.J., Preisinger, A.C., Jessup, J.M., Paraskeva, C., Markowitz, S., Willson, J.K., Hamilton, S., and Vogelstein, B. (1990). p53 gene mutations occur in combination with 17p allelic deletions as late events in colorectal tumorigenesis. Cancer Res. *50*, 7717–7722.

S3. Jacobs, J.J., Kieboom, K., Marino, S., DePinho, R.A., and van Lohuizen, M. (1999). The oncogene and Polycomb-group gene bmi-1 regulates cell proliferation and senescence through the ink4a locus. Nature *397*, 164–168.

S4. Dimri, G.P., Martinez, J.L., Jacobs, J.J., Keblusek, P., Itahana, K., Van Lohuizen, M., Campisi, J., Wazer, D.E., and Band, V. (2002). The bmi-1 oncogene induces telomerase activity and immortalizes human mammary epithelial cells. Cancer Res. *62*, 4736–4745.

S5. Brummelkamp, T.R., Bernards, R., and Agami, R. (2002). Stable suppression of tumorigenicity by virus-mediated RNA interference. Cancer Cell *2*, 243–247.

S6. Voorhoeve, P.M., and Agami, R. (2003). The tumor-suppressive functions of the human INK4A locus. Cancer Cell *4*, 311–319.

S7. Narita, M., Nunez, S., Heard, E., Lin, A.W., Hearn, S.A., Spector, D.L., Hannon, G.J., and Lowe, S.W. (2003). Rb-mediated heterochromatin formation and silencing of E2F target genes during cellular senescence. Cell *113*, 703–716.

S8. Zhu, X.D., Kuster, B., Mann, M., Petrini, J.H., and de Lange, T. (2000). Cell-cycle-regulated association of RAD50/MRE11/NBS1 with TRF2 and human telomeres. Nat. Genet. *25*, 347–352.

S9. Dimri, G.P., Lee, X., Basile, G., Acosta, M., Scott, G., Roskelley, C., Medrano, E.E., Linskens, M., Rubelj, I., Pereira-Smith, O., et al. (1995). A biomarker that identifies senescent human cells in culture and in aging skin in vivo. Proc. Natl. Acad. Sci. USA *92*, 9363–9367.

S10. Herbig, U., Jobling, W.A., Chen, B.P., Chen, D.J., and Sedivy, J.M. (2004). Telomere shortening triggers senescence of human cells through a pathway involving ATM, p53, and p21(CIP1), but not p16(INK4a). Mol. Cell *14*, 501–513.

S11. Alkema, M.J., Bronk, M., Verhoeven, E., Otte, A., van 't Veer, L.J., Berns, A., and van Lohuizen, M. (1997). Identification of Bmi1-interacting proteins as constituents of a multimeric mammalian polycomb complex. Genes Dev. *11*, 226–240.

S12. van Steensel, B., Smogorzewska, A., and de Lange, T. (1998). TRF2 protects human telomeres from end-to-end fusions. Cell *92*, 401–413.